DEVELOPMENT OF A DIELECTRIC SPECTROMETER PROBE FOR CHARGE AND SIZE ANALYSIS OF INDUSTRIAL SLURRIES

Final Technical Report

Philip Goetz
Pen Kem, Inc.
341 Adams St
Bedford Hills, NY

January, 2003

DISCLAIMER

DISCLAIMER

Portions of this document may be illegible in electronic image products. Images are produced from the best available original document.

Summary

DEVELOPMENT OF A DIELECTRIC SPECTROMETER PROBE FOR CHARGE AND SIZE ANALYSIS OF INDUSTRIAL SLURRIES

Dr. Hemant Pendse, Project Manager, P&G Systems, Inc.
Mr. Philip J. Goetz, Principle Investigator, Pen Kem, Inc.

The project focus is on the design of a small and robust remote sensor probe to meet the as yet unmet needs of industry to characterize the charge and size of colloidal dispersions (suspensions and emulsions). Such dispersions may have high particle concentration with submicron sized particles and are therefore unsuitable for optical methods. Many dispersions of interest also have particles with low density contrast which makes them unsuitable for ultrasonic analysis. Our approach combines rapid measurements of dielectric spectra of the colloid with a deconvolution of the measured spectra to obtain size distribution and charge.

A microsensor for simultaneous charge and size analysis of colloidal dispersions commonly encountered in industrial processing has been designed for a dielectric spectroscopy probe. Measured dielectric spectra were interpreted in terms of existing theories of various polarization processes. Several designs have been evaluated and two prototypes were built. An extensive literature review on non-equilibrium electric surface phenomena relevant to colloidal dispersions was done.

During Phase 11 we improved and extended the probe design and developed new deconvolution algorithms using the real and imaginary parts of the measured spectra. Some advances in the theoretical understanding of underlying polarization phenomena were made to address many dispersions of practical interest, for example, the accounting of the effects of high particle concentrations. Tests were performed using both model and industrial colloids to evaluate the performance of the micro sensor probes, new theoretical relationships, and new deconvolution algorithms.

DEVELOPMENT OF A DIELECTRIC SPECTROMETER PROBE FOR CHARGE AND SIZE ANALYSIS OF INDUSTRIAL SLURRIES

Table of Contents

1 Background

A brief general background on dielectric spectroscopy in the context of obtaining charge and size information for colloidal dispersions is as follows:

1. Dielectric spectroscopy involves monitoring the frequency-dependent real and imaginary parts of the complex electrical conductivity (or equivalently the complex admittance or complex dielectric permittivity) of a colloid dispersion. This response is very rich in information regarding the particle size distribution, particle volume fraction, the total diffuse charge density or Stern potential, the adsorbed ion charge density, and the ion binding characteristics. Figure 1 shows a schematic illustrative of the data.

2. Unlike various methods based on electrokinetic phenomena, dielectric spectroscopy enables one to characterize the total diffuse charge (or Stern potential) as well as the adsorbed charge. The electrokinetic charge is only a part of the total diffuse charge and thus the electrokinetic (or zeta) potential is not always a good approximation of the Stern potential, especially for real surfaces which are rough and not molecularly smooth, or may be porous or hairy. Particle-particle and particle-ion interactions are governed by the Stern potential and not the zeta potential. To date, the analysis of the Stern potential has been limited due to the lack of convenient instrumentation. A schematic representation of the electric double layer around a colloidal particle, and the associated potential distribution, is shown in Figure 2.

3. The relaxation frequency characteristic of the dielectric response, as given in Figure 3, is known to be inversely proportional to the square of the particle radius. We can use the entire dielectric spectra to obtain particle size distribution using various deconvolution methods.

4. We can combine typical kHz-frequency ($< f_{D-Sh}$) dielectrometry with MHz-frequency ($> f_{D-Sh}$) conductometry so as to cover a wide range of the relaxation parameter values characterizing the ratio of the surface conduction to the bulk conduction. On the other hand, dielectric measurements at very high GHz-frequencies ($\sim f_{m-w}$) are mainly governed by particle concentration rather than size and charge characteristics, and are thus less useful for us.
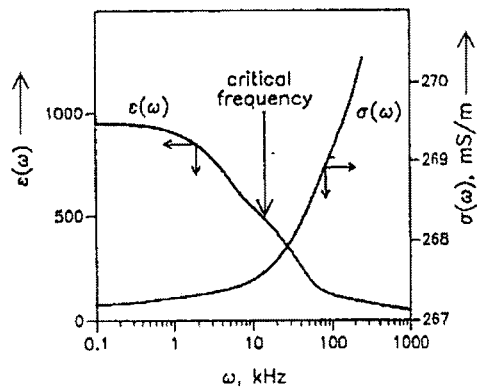
5. The existing theory of dielectric spectroscopy is suitable for the case of non-conducting particles at low volume fraction, with fixed surface charge and weakly adsorbing counter-ions in aqueous binary electrolyte solutions. This theory is mainly based on the 1974 Dukhin-Shilov analysis. Although few other academic researchers' world-wide have extended computational applications of this theory, efforts to date have been mainly focused on its experimental verification.

6. Our team (Prof Pendse and Prof Dukhin) has formulated approaches for extensions to account for the effects of particle concentration, adsorbed counter-ion polarization and mobile surface charges.

- Frequency Response of Complex
  Conductivity, K^*

$$K^*(\omega) \equiv K'(\omega) + jK''(\omega)$$

$$K^*(\omega) = \sigma(\omega) + j\omega\varepsilon_0\varepsilon(\omega)$$

- Relaxation of Ionic Atmosphere
  Under Alternating Electric Fields

All charges bulk as well as
⊞ + diffuse,
⊕   adsorbed, and
⊖   surface
may participate in polarization

- Measurements of complex
conductivity as a function of frequency,
$K^*(\omega)$, are very rich in information

$$K^*(\omega) \sim a, \; \kappa^{-1},$$
$$D_{bulk}, \; D_{diff}, \; D_{ads}, \; D_{surface},$$
$$\sigma_d, \; \sigma_a,$$
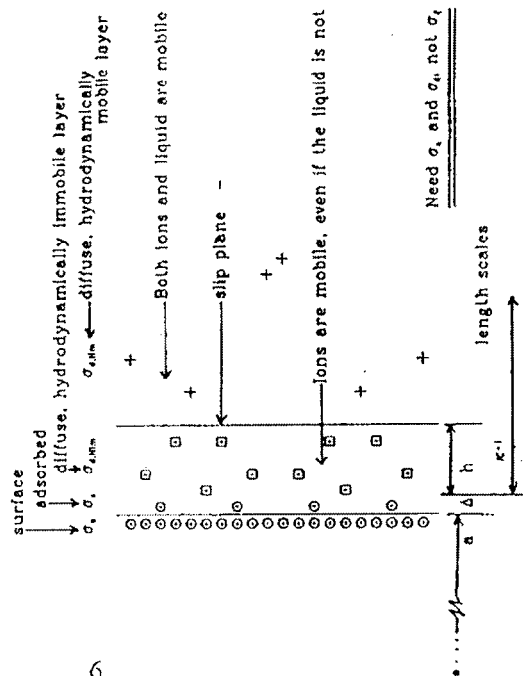$$\psi_d, \; \zeta$$

Figure 1

Figure 2

- Electrical Double Layer Around a Colloid Particle

$$\sigma_s = \sigma_a + (\sigma_{d,Hlm} + \sigma_{d,Hm})$$

$$\sigma_s = \sigma_a + \sigma_d + \sigma_\zeta$$

surface adsorbed diffuse electrokinetic

surface
adsorbed
diffuse, hydrodynamically immobile layer $\sigma_{d,Hlm}$
diffuse, hydrodynamically mobile layer

Both ions and liquid are mobile

slip plane

Ions are mobile, even if the liquid is not

Need σ_a and σ_d, not σ_ζ

length scales

- Potential Distribution Around a Colloid Particle

Surface Charge
$\sigma_s = \sigma_a + \sigma_d$
Adsorbed Charge

Total Diffuse Charge
$\sigma_d = \sigma_{d,Hlm} + \sigma_{d,Hm}$
σ_ζ
Electrokinetic Charge
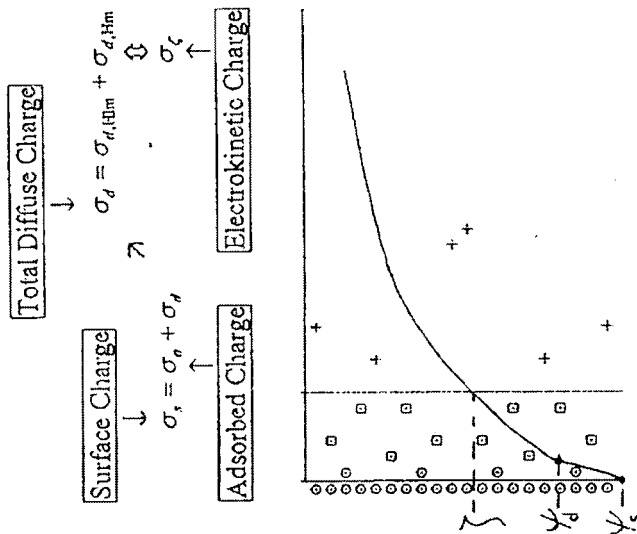
6

Figure 3

- ## A Closer Look at the Critical Frequency, f_c

$$f_c \sim \frac{D_{\text{bulk}}}{a^2} \qquad \text{concentration polarization}$$

(Dukhin-Shilov)

$$\sim \frac{D_{\text{bulk}}}{\kappa^{-2}} \qquad \text{Maxwell-Wagner}$$

polarization

$$\sim \frac{D_{\text{ads}} f(\sigma_a, \psi_d)}{a^2} \qquad \text{bound ion polarization}$$

(Schwarz)

7

2 Theory

There are two frequency regions where dielectric permittivity changes with frequency. The KHz range usually corresponds to "low frequency dielectric dispersion". In this range the characteristic frequency depends on the particle size and diffusion coefficient:

Equation 1

$$f_{low} = \frac{\pi D}{a^2}$$

The high frequency dielectric dispersion lies in the MHz range. It is referred to as Maxwell-Wagner dispersion. This Maxwell-Wagner frequency depends on conductivity K and permittivity ε of the medium, or on ratio of the Debye length and diffusion coefficient

Equation 2

$$f_{MV} = \frac{K}{\varepsilon \varepsilon_0} = \chi^2 D$$

In principle, the low frequency dispersion looks more attractive as a characterization technique because it opens an opportunity to characterize at the same time both particle size and surface properties. For this reason we concentrated the efforts of the theoretical group, lead by Prof Dukhin, on the theory of the low frequency dispersion. This group achieved significant progress in the theory of the low frequency dispersion, resulting in eight published papers. However, a critical analysis of these works shows that low frequency dielectric dispersion is too complicated a phenomenon to be used in any robust and technically simple characterization technique.

There is an additional argument against using low frequency dispersion in a commercial dielectric spectrometer. Measurements in the low frequency range are much more complicated because of electrode polarization.

Keeping in mind these arguments, we decided to concentrate our efforts on the Maxwell-Wagner high frequency dispersion. The theory of for high frequency dispersion is fairly well known and tested. A "cell model" implementation of this theory allows it to be applied to concentrated colloids. It was expanded for charged particles in conducting media by O'Konski. However, all of the existing theory made the monodisperse assumption that all particles had the same size. We needed to expand the existing theory to allow for practical polydisperse systems by adding one additional parameter to the model.

3 Cell Model for a Polydisperse System

The main idea of the "cell model" is that each particle in a concentrated system is considered separately inside a spherical cell of liquid associated only with this individual particle. The cell boundary conditions formulated on the outer boundary of the cell reflect the particle-particle interaction.

In the past, the cell model has been applied only to monodisperse systems. This restriction allows one to easily define the radius of the cell. Equating the solid volume fraction of each cell to the volume fraction of the entire system yields the following expression for the cell radius b:

Equation 3

$$b = \frac{a}{\sqrt[3]{\varphi}}$$

In the case of a polydisperse system, the introduction of the cell is more complicated because the liquid can not be distributed between fractions in an infinite number of ways. However, the condition of mass conservation is still necessary.

Each fraction can be characterized by particles radii a_i, cell radii b_i, thickness of the liquid shell in the spherical cell $h_i = b_i - a_i$ and volume fraction φ_i. The mass conservation law relates these parameters together as follows:

Equation 4

$$\sum_{i=1}^{N} \left(1 + \frac{h_i}{a_i} \right)^3 \varphi_i = 1$$

Expression (3.2) might be considered as an equation with N unknown parameters h_i. An additional assumption is still necessary to determine the cell properties for the polydisperse system. This additional assumption should define the relationship between particle radii and shell thickness for each fraction. We suggest the following simple relationship:

Equation 5

$$h_i = h_{a_i^n}$$

This assumption reduces the number of unknown parameters to only two which are related by the following expression:

Equation 6

$$\sum_{i=1}^{N} \left[1 + h_{a_i^{n-1}} \right]^3 \varphi_i = 1$$

It is convenient to calculate the values of the **h** for the various values of n. The parameter n will be referred to as a "shell factor". Two specific values of the shell factor correspond to easily understood cases. A shell factor of zero depicts the case in which the thickness of the liquid layer is independent on the particle size. A shell factor of 1 corresponds to the normal "superposition assumption" which gives the same relationship between particles and cell radiuses in the monodisperse case, i.e. each particle is surrounded by a liquid shell which provides each particle the same volume concentration as the volume concentration of the overall system. In general, the "shell factor" is considered an adjustable parameter because it adjusts the dissipation of energy within the cells.

4 Maxwell-Wagner-O'Konski theory

The theory of a dispersed system dielectric permittivity and conductivity within MHz frequency range has been created by Maxwell, Wagner, and O'Konski. Later O'Brien shown that "cell model" leads to the same results. This theory gives the following expression for the complex dielectric permittivity:

• **Equation 7**

$$\varepsilon^* = \frac{1 - 2\varphi F^*}{1 + \varphi F^*}$$

where φ is the volume fraction and function F* equals to:

• **Equation 8**

$$F^* = \frac{K_m^* - K_p^*}{2K_m^* + K_p^m}$$

and:

$$K^* = K + jw\varepsilon$$

$$K_m^* = K_m + jw\varepsilon_m$$

$$K_p^* = K_p + jw\varepsilon_p + \frac{2\chi^\sigma}{a}$$

$$K^* = jw\varepsilon^*$$

$$\alpha = \frac{wa^2}{\nu}$$

$$w = 2\pi f$$

where K and ε, K_m and ε_m, K_p and ε_p are conductivities and dielectric permitivities of the disperse system, dispersion medium and disperse phase respectively, η and ν are the dynamic and kinematic viscosities of the medium, χ^σ is a surface conductivity, f is the frequency in Hz.

The real part of ε^* is a real dielectric permittivity, whereas imaginary part is the real conductivity of the dispersed system.

The dielectric permittivity and conductivity frequency spectra contain information about electric surface properties because function F* depends on the value of the so-called Dukhin number Du, given by:

Equation 9

$$Du = \frac{2\chi^\sigma}{K_m a} = \frac{e^{\left(\frac{e\psi_d}{2kT}\right)}}{\chi^a}$$

Software was written implement these theories and thereby predict the complex conductivity of any given colloid in terms of the zeta potential, particle size and other physical properties of the system. A typical computed dielectric permittivity and conductivity spectra are shown in Figure 4. Such a prediction program is the first step in developing a deconvolution program for solving the inverse problem, namely computing the zeta potential and particle size given a measured complex conductivity spectra.
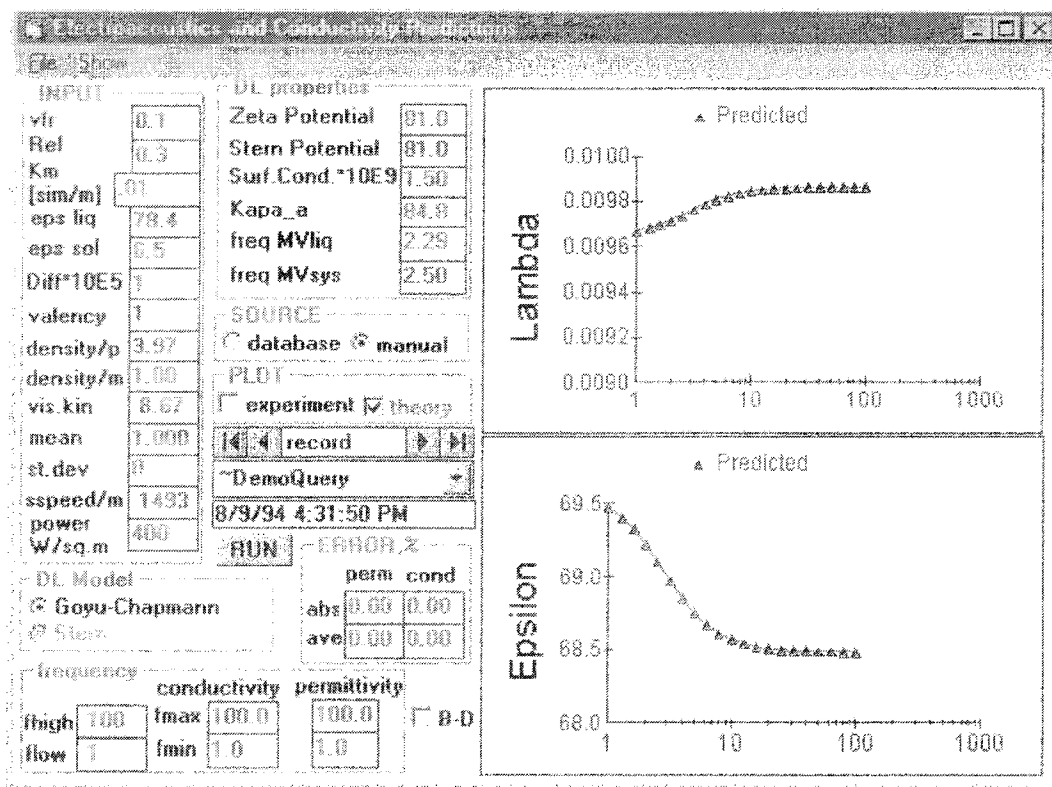

Figure 4 Predicted complex conductivity spectra for 1 micron size particles with zeta potential of 81 mV

5 Measuring Technique

A measuring instrument suitable for measuring in both the low frequency and high frequency region was developed that employed a planar four electrode interdigitated sensor in combination with a commercially available HP network analyzer. A simplified block diagram of the instrument is shown in Figure 5. The Electronics measuring unit, i.e. the HP network analyzer, provides the excitation to the probe. The sensor current is measured with an op-amp configured as a current sensor. The voltage is measured with a second set of sensing electrodes and buffered by a second high impedance FET op amp to minimize any circuit loading.

The actual construction of the planar probe is shown in Figure 6. It is fabricated on low loss printed circuit board, the electrodes being photo etched on the surface and subsequently gold plated to provide a chemically stable probe.
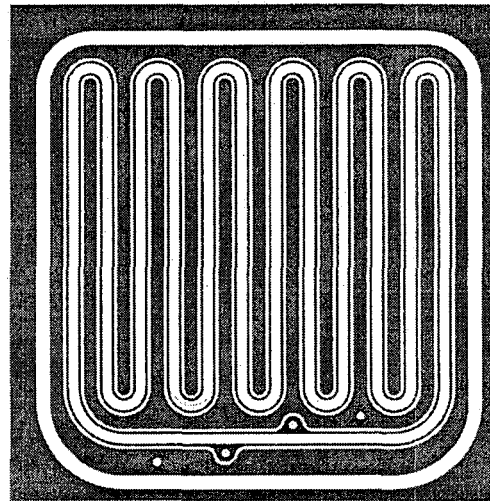

Figure 5 Block diagram of wide band sensor

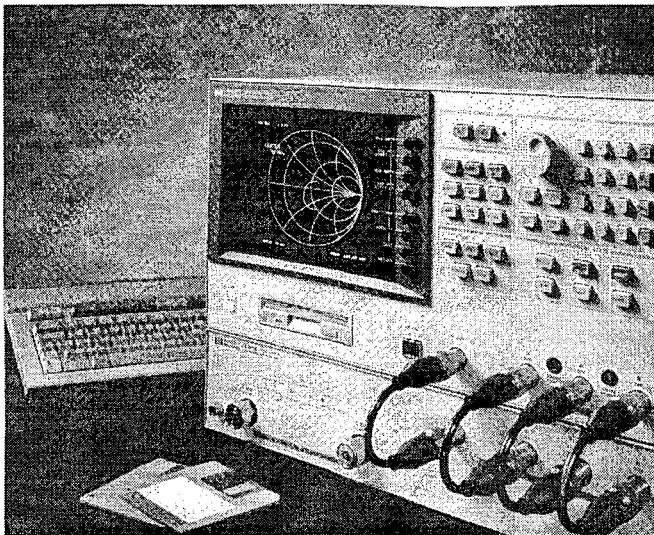**Figure 6 Four electrode sensor probe**

Figure 7 HP Network Analyzer used for EMU

For test purposes, the actual sensor probe was initially replaced by a lumped circuit that simulates the complex conductivity of a typical colloid.
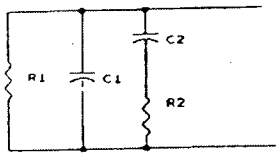

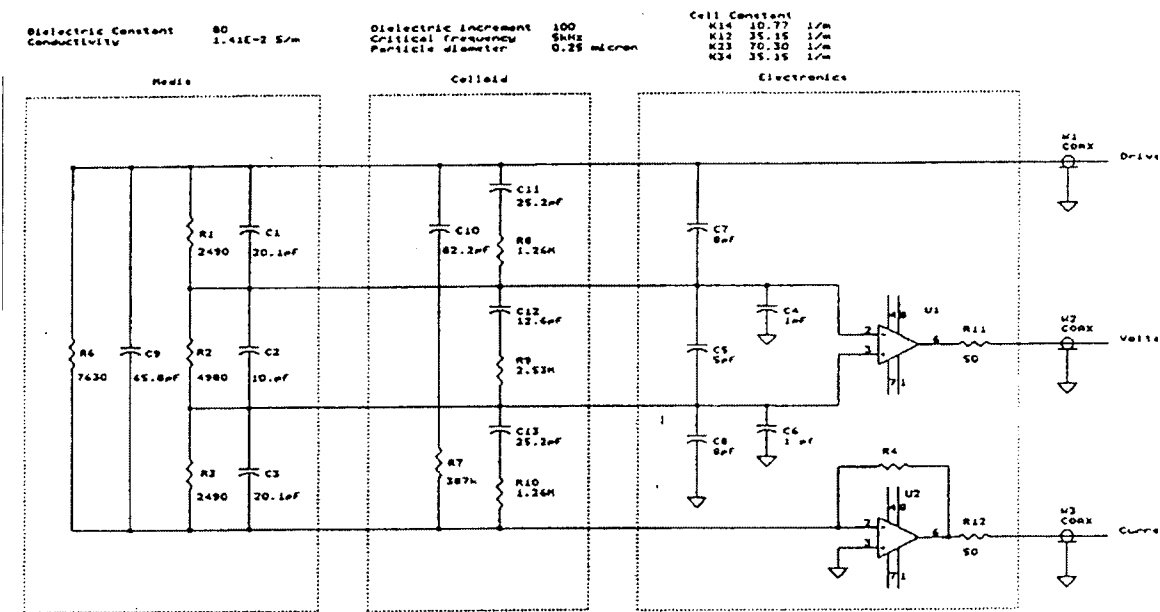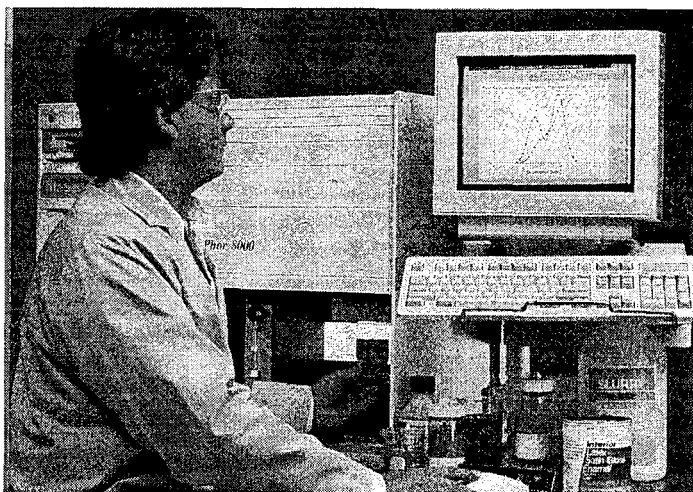**Fig 7 Lumped element analog of typical colloid**

Figure 8 Lumped element model of four electrode sensor, colloid, and measuring circuit

Results show that a frequency-dependent dielectric response of colloidal systems can be monitored very rapidly, typically 64 point scans over a frequency range from 5 Hz to 1 MHz in 15 seconds. We tested our flat probe with the inter-digitated electrodes in a simple cup using a variety of KCl-Water solutions.

As mentioned earlier, as a result of our analysis we decided to concentrate effort in the higher frequency range. At the same time, we wanted to move towards a commercial implementation of the device. Accordingly we fabricated a simpler probe and replaced the network analyzer, capable of measurements from 5Hz to 500 MHz, with a modified Pen Kem Acoustophor 8000, which was capable of measurements over a limited range of 1 to 100 MHz. The Acoustophor 8000, depicted in Figure 9, is a pulse based system, in contrast to the CW technique employed by the HP network analyzer. The software automatically adjusts the number of collected pulses in order to achieve a specified signal-to-noise ratio. The system response is linear because of the low signal power, about 10 mW.

Construction of the dielectric probe reflects the requirements of minimizing parasite currents and of performing reproducible measurements. Our equivalent scheme, depicted in Figure 8, contains 4 capacitors, 4 resistors and 2

inductance and appropriate geometric cell constants. We have developed a program which calculates transfer function of this equivalent circuit. This program interface is shown on Figure 4 Calibration Program.

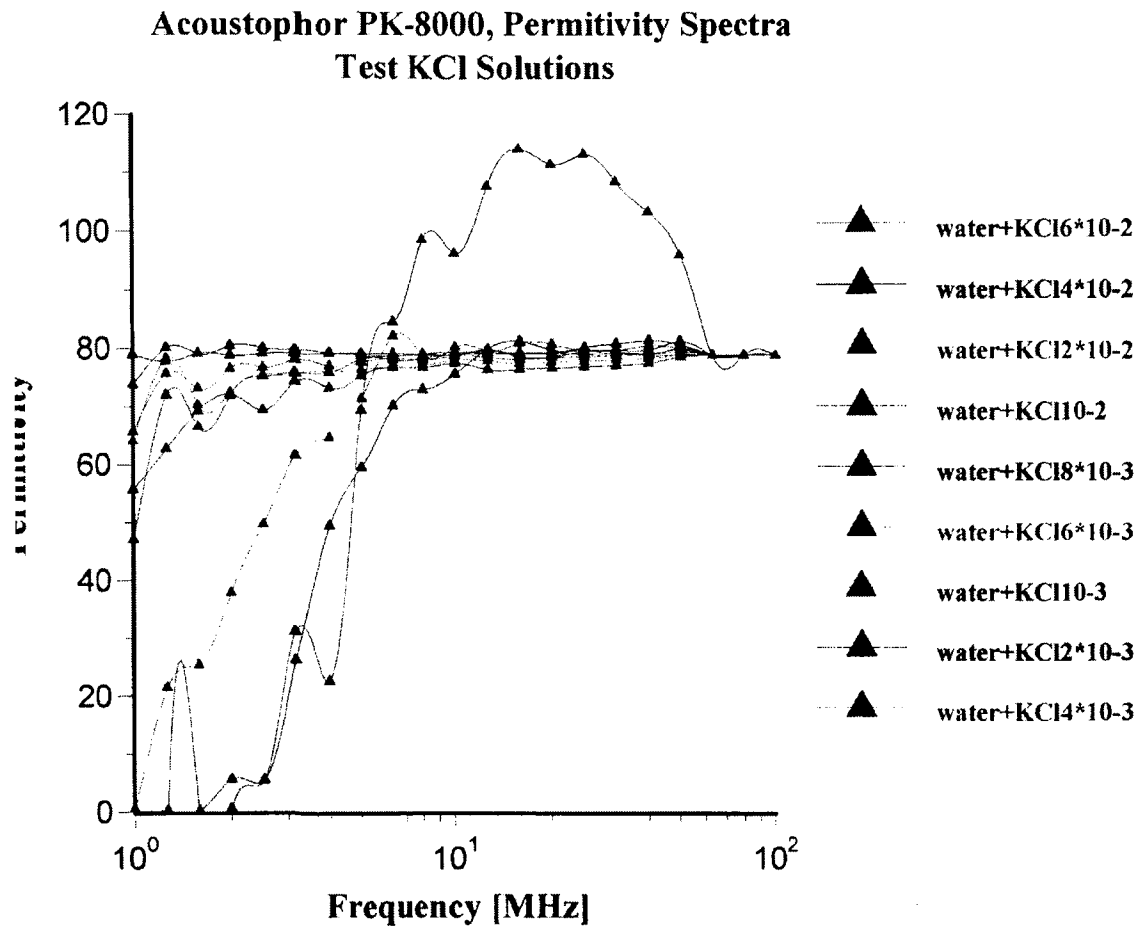**Figure 9   Pen Kem Acoustophor 8000 modified for Dielectric Spectroscopy work**

A special three steps calibration procedure makes it possible to determine unknown parameters of the equivalent scheme. This calibration procedure includes measurement performed with short circle, open circle and chamber filled with known aqueous KCl solution. Each measurement gives frequency dependence of real and imaginary parts of the total transfer function. Minimization of the deviation between calculated and measured transfer function makes it possible to determine all unknown parameters.

There is logical test to verify this approach. A set of the various KCl solutions with different known conductivities can be used first for calibration and then for measurement. This consistency test clarifies the frequency and conductivity range where the above approach is valid.

Results of this test are shown in Figure 10 and 11. It is seen that this method permits measurement of both conductivity and permittivity for the full frequency range from 1 to 100 MHhz if the conductivity is more than 10-3 mol/l KCl and less than 10-2 mol/l KCL.
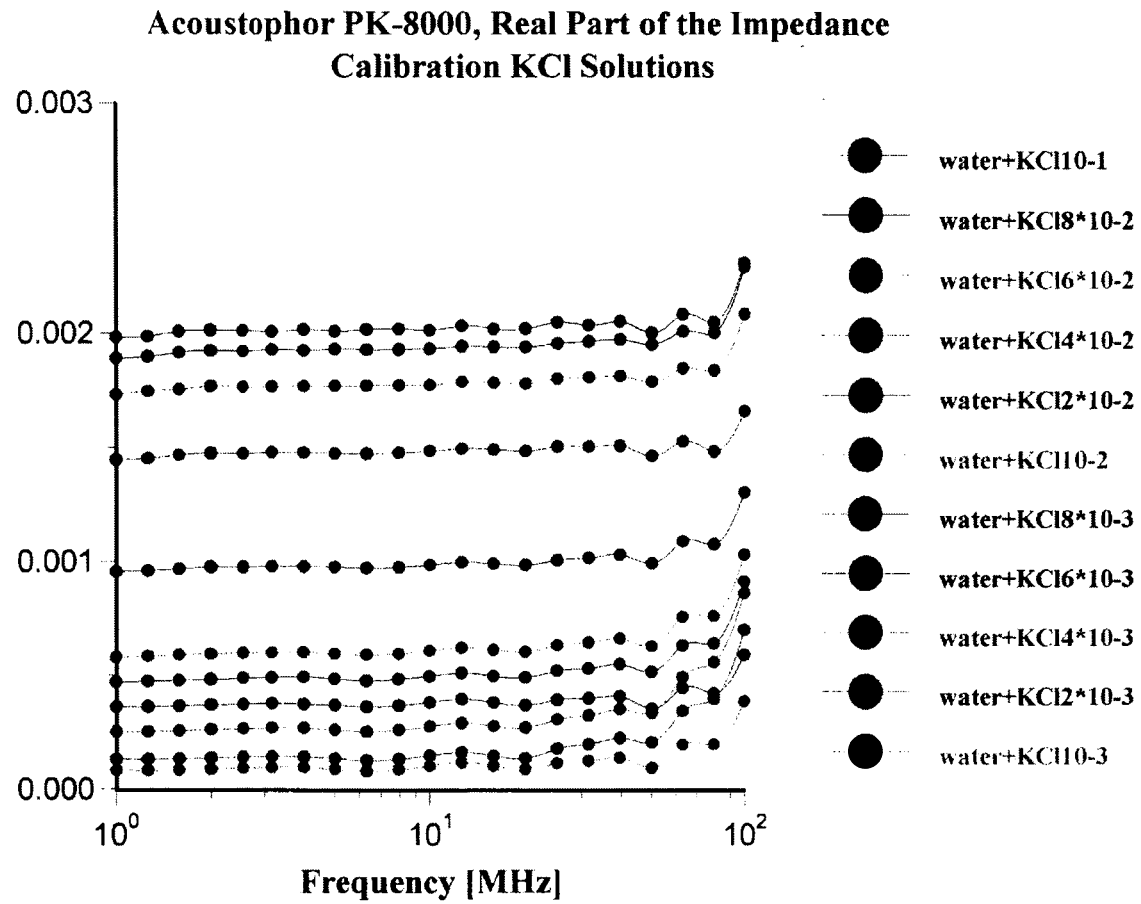
Figure 10 Dielectric constant for various KCL standards

Acoustophor PK-8000, Permitivity Spectra
Test KCl Solutions

/29/96 19:33:51 Graph4

Figure 11 Conductivity spectra for various KCL standards

Acoustophor PK-8000, Real Part of the Impedance Calibration KCl Solutions

Legend:
- water+KCl10-1
- water+KCl8*10-2
- water+KCl6*10-2
- water+KCl4*10-2
- water+KCl2*10-2
- water+KCl10-2
- water+KCl8*10-3
- water+KCl6*10-3
- water+KCl4*10-3
- water+KCl2*10-3
- water+KCl10-3

Frequency [MHz]

/29/96 19:14:15 Graph1

16

6 Results and Discussion

We have tested the dielectric spectrometer with a Geltech 10% wt % aqueous silica dispersion, having a mean particle size of 0.5 micron and a fairly monodisperse distribution. We prepared seven samples at different pH from 3.9 to 10. The goal of this test was to prove that dielectric spectrometer is sensitive to the changes in the surface properties, i.e. we could determine the zeta potential from the measured spectra.

The results of these measurements are shown on the 12-18. On each figure the somewhat noisy curve presents the experimental data, whereas the smooth curve represents the best theoretical fit of our prediction model to this data.

The dielectric permittivity of the all seven samples is significantly lower than the dielectric permittivity of pure water. We measure a value of about 70 for the slurry, whereas the permittivity of pure water at room temperature is about 80. This decrease in the dielectric permittivity reflects presence of the silica particles with their lower dielectric constant. This experimental result confirms that the dielectric spectrometer is sensitive to the presence of the disperse particles. The resulting permittivity and conductivity spectra contain useful information concerning the size and zeta potential of the particles.
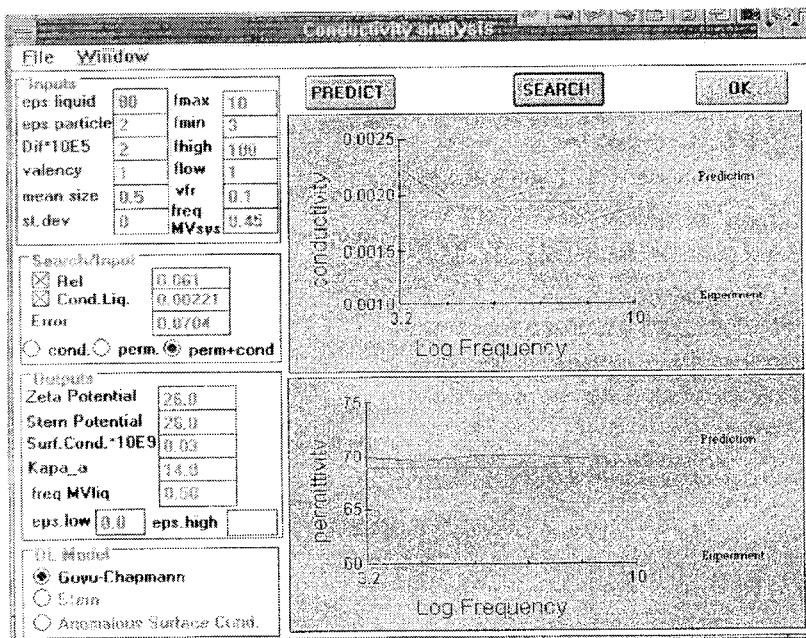
Finally, Figure 19 illustrates dependence of the calculated zeta potential on the pH of the sample. It is seen that the zeta potential decreases with a decrease of pH as is typical for a silica slurry.

This titration experimental test proves that dielectric spectrometer can be used for characterization of the colloid surface properties. At the same time we should note that this measured permittivity and conductivity spectra are till somewhat noisy. In addition, there is sometimes the problem of multiple solutions, which is to say that there are several combinations of parameters leading to the same quality of fit between the prediction model and the experimental spectra. Performance of the measuring device needs to be further improved in order to reach the necessary precision that would be sufficient for guaranteeing a unique solution.
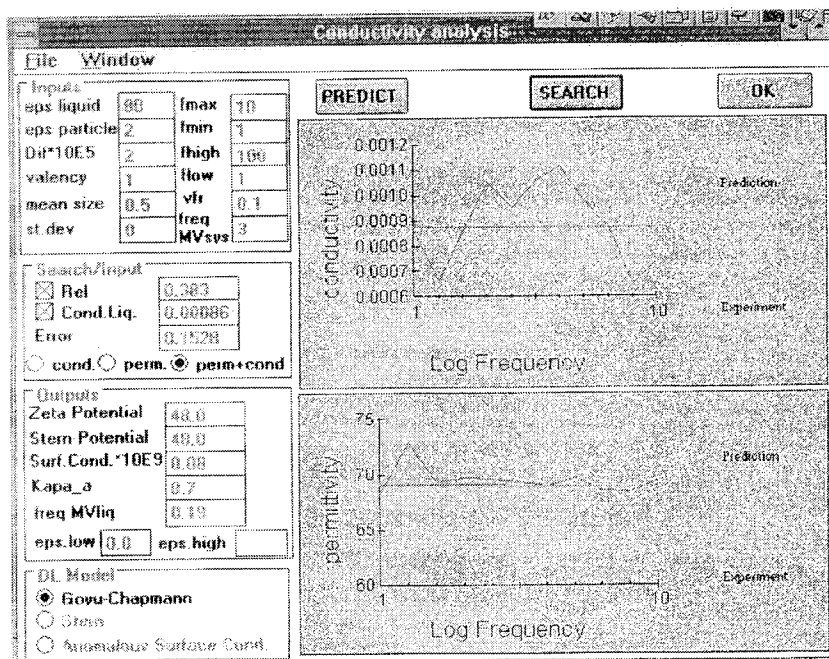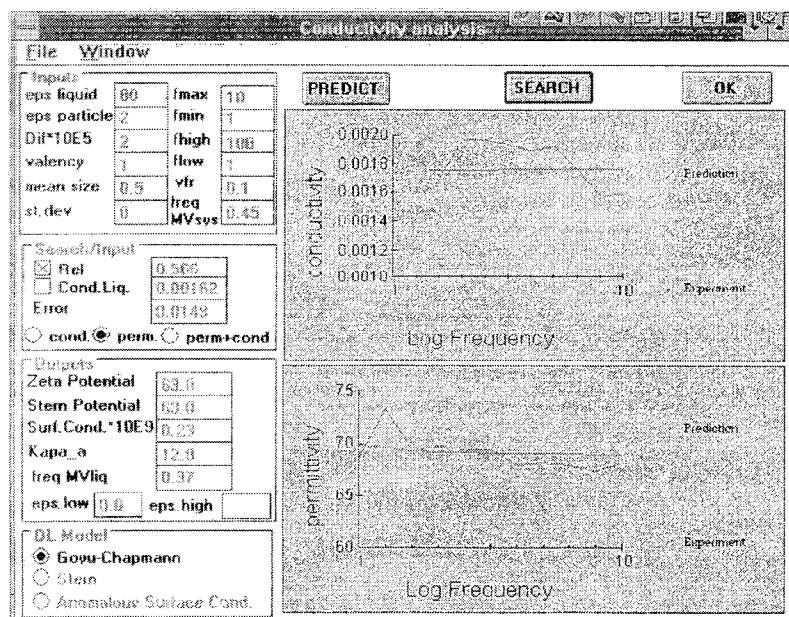
Figure 12 Dielectric spectra at pH 3.9

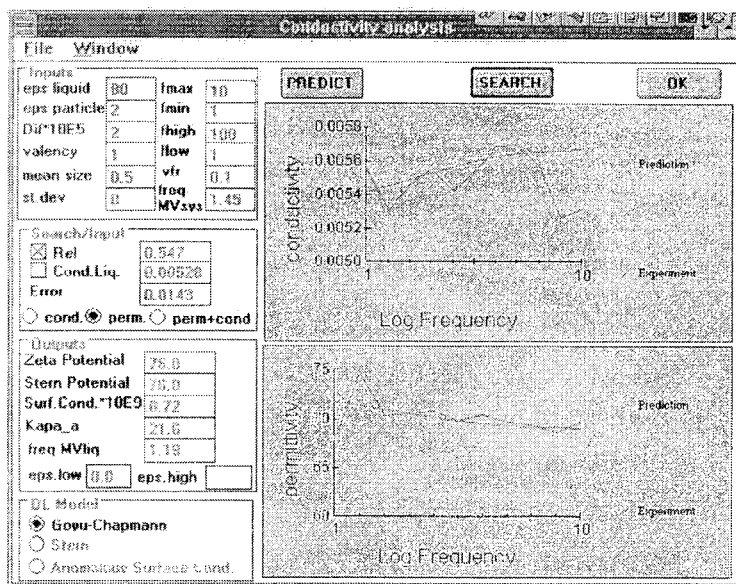**Figure 13 Dielectric spectra at pH 5**

silica 10%vl, pH=5.9

Figure 1 Dielectric spectra at pH 5.9

silica 10%vl, pH=7

Figure 2 Dielectric spectra at pH 7

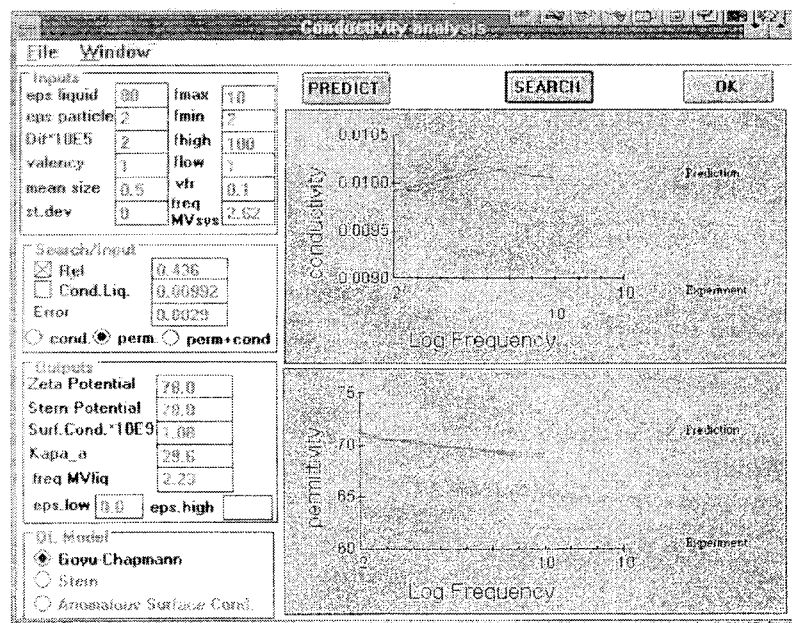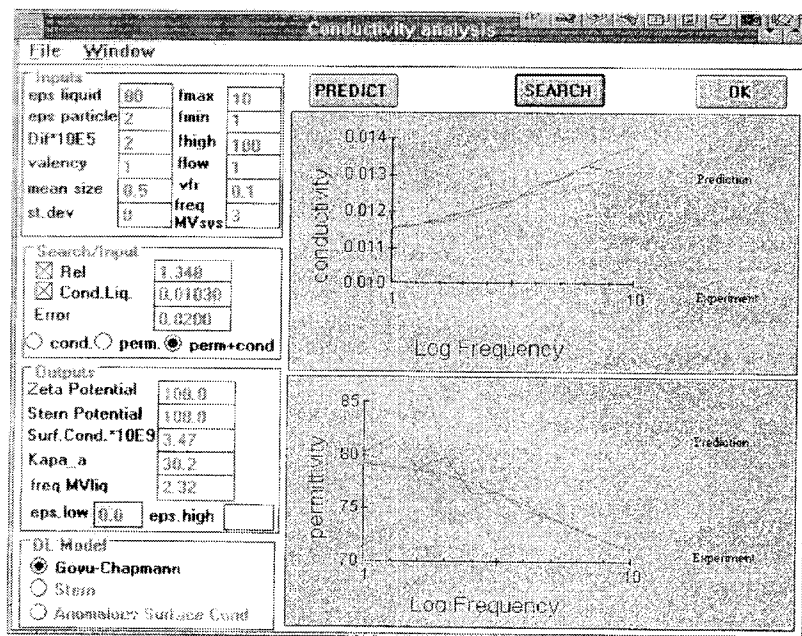silica 10%vl, pH=8.2

Figure 3 Dielectric spectra at pH 8.2

silica 10%vl, pH=9.1

Figure 4 Dielectric spectra at pH 9.1

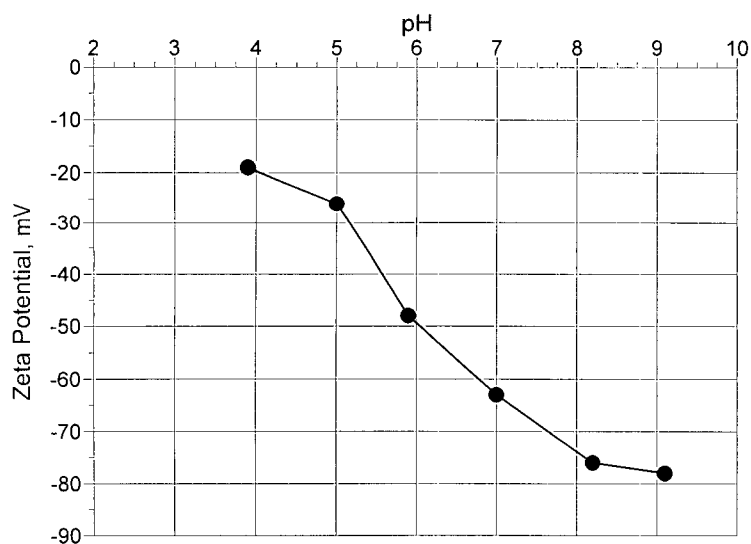**Figure 5 Dielectric spectra at pH 10**

Figure 19 Zeta potential of silica slurry computed from dielectric spectra